Published in final edited form as:
J Immunol. 2015 February 15; 194(4): 1776–1787. doi:10.4049/jimmunol.1401684.

High-mobility group box 1: A novel target for treatment of *Pseudomonas aeruginosa* keratitis

Sharon McClellan, **Xiaoyu Jiang**, **Ronald Barrett**, and **Linda D. Hazlett**
Department of Anatomy & Cell Biology, Wayne State University School of Medicine, Detroit, MI 48201

Abstract

High mobility group box 1 (HMGB1), a prototypic alarmin, mediates the systemic inflammatory response syndrome. Treatment with vasoactive intestinal peptide (VIP), an anti-inflammatory neuropeptide, down-regulates pro-inflammatory cytokines and promotes healing in a susceptible (cornea perforates) model of *Pseudomonas (P.) aeruginosa* keratitis, also significantly down-regulates HMGB1 expression. Therefore, we examined targeting HMGB1 for treatment of *P. aeruginosa* keratitis to avoid delivery and other issues associated with VIP. For this, HMGB1 was silenced using siRNA, while controls were treated with a non-specific scrambled sequence siRNA. Less disease was seen after infection in siHMGB1 over control mice and was documented by clinical score and photographs with a slit lamp. Real time RT-PCR and ELISA confirmed HMGB1 knockdown. RT-PCR analysis also revealed reduced mRNA levels of IL-1β, MIP-2, TNF-α, TLR4, and receptor for advanced glycation end products (RAGE), while mRNA levels of anti-inflammatory TLRs SIGIRR and ST2 were significantly increased. HMGB1 knockdown also decreased IL-1β and MIP-2 proteins, reducing PMN number in the infected cornea. mRNA and protein levels of CXCL12 and CXCR4, as well as mononuclear cells, were significantly reduced after HMGB1 knockdown. Antibody neutralization of HMGB1, infection with a clinical isolate and rHMGB1 treatment of resistant mice, supported the silencing studies. These data provide evidence that silencing HMGB1 promotes better resolution of *P. aeruginosa* keratitis by decreasing levels of pro-inflammatory mediators, (decreasing PMN infiltration), increasing anti-inflammatory TLRs, reducing CXCL12 (preventing HMGB1/CXCL12 heterodimer formation), and signaling through CXCR4, reducing monocyte/macrophage infiltration.

Introduction

Pseudomonas aeruginosa (*P. aeruginosa*), an opportunistic Gram-negative pathogen, is one of the most common causes of microbial keratitis in extended wear contact lens users and those who are immunocompromised (1). Both host derived and bacterial factors contribute to the rapidly progressing disease marked by inflammatory epithelial edema and infiltration of the stroma by PMN and mononuclear cells (2). Animal models of bacterial keratitis, including the mouse model used in this laboratory, have provided data that rapid recruitment of PMN (3) to the infected cornea is necessary to control bacterial load, however, failure to

Corresponding Author: Linda D. Hazlett, Ph.D., Department of Anatomy & Cell Biology, Wayne State University School of Medicine, 540 E. Canfield Avenue, Detroit, MI 48201, Phone: (313) 577-1079, lhazlett@med.wayne.edu, Fax: (313) 577-3125.

regulate their persistence/removal, can result in stromal damage, scarring and/or ultimately, loss of vision (4–7). Many cytokines and chemokines influence the migration of PMN and/or mononuclear cells into tissues, including but not limited to, IL-1β, MIP-2 (mouse homologue of IL-8) and CXCR4 signaling. Susceptible (cornea perforates) C57BL/6 mice significantly up-regulate both of the former two cytokines after infection, compared to levels in the resistant (cornea heals) BALB/c mouse (8–9). In that regard, vasoactive intestinal peptide (VIP) is an anti-inflammatory neuropeptide that has been shown to promote resistance against *P. aeruginosa* keratitis in the susceptible C57BL/6 mouse (10). One of the mechanisms by which this is achieved is its ability to down-regulate expression of IL-1β and MIP-2 in the cornea resulting in significantly less PMN infiltration following infection (10). In addition, VIP treatment also was shown to reduce several TLR related molecules in the infected cornea of C57BL/6 mice (11) that also were reduced systemically in a model of sepsis (12). Despite these encouraging data, the key to the successful therapeutic use of VIP in human disease remains problematic, particularly because of difficulty with its delivery (13). Thus, it was of interest to us that in other studies, (12) the therapeutic effect of VIP was accompanied by a decrease in systemic levels of the alarmin, HMGB1 and the protective effects of VIP could be abrogated by rHMGB1 treatment (12). HMGB1 is a well-studied alarmin that is expressed in nearly all cell types. Injury or infection results in its release and subsequent binding to mediators of inflammation such as TLR2, 4, 9, or RAGE and activation of innate and adaptive immunity (13). Most importantly, antagonistic HMGB1 treatment, including use of antibodies, antagonists, and pharmacological agents, has proven successful in many pre-clinical inflammatory disease models, reducing disease severity and lethality (13–15).

Thus, the current study examined the effects of silencing HMGB1 in bacterial keratitis. We provide evidence that knockdown of HMGB1 expression by RNA interference in the susceptible C57BL/6 mouse results in protection of the infected cornea from perforation. Silencing of HMGB1 also reduced mRNA levels of pro-inflammatory, while up-regulating expression of anti-inflammatory cytokines. Protein levels of IL-1β and MIP-2 also were significantly lower in the infected cornea after siHMGB1 compared to scrambled control treatment and correlated with reduced PMN in cornea. Reduction in CXCL12, preventing HMGB1/CXCL12 heterodimer formation and reduced signaling through CXCR4 was also observed following siHMGB1 treatment and contributed to reduced mononuclear cell infiltration. Selectively testing antibody neutralization and infection with a clinical isolate in C57BL/6 mice provided supportive data. In addition, increasing alarmin levels by treating BALB/c (resistant) mice with rHMGB1, not only enhanced the PMN infiltrate but resulted in worsened disease. Collectively, the data suggest that reducing HMGB1 expression and signaling, may provide an alternate approach to improve disease outcome in microbial keratitis.

Materials and Methods

Mice

Female 8 week old C57BL/6 and BALB/c mice were purchased from the Jackson Laboratory (Bar Harbor, ME) and housed in accordance with the National Institutes of

Health guidelines. The animals were treated humanely in accordance with the Association for Research in Vision and Ophthalmology Statement for the Use of Animals in Ophthalmic and Vision Research.

Bacterial culture and infection

P. aeruginosa strain 19660 (American Type Culture Collection, Manassas, VA) and clinical isolate KEI 1025 (Kresge Eye Institute, Detroit, MI) were grown in peptone tryptic soy broth at 37°C in a reciprocal shaking water bath at 150 rpm for 18h. Bacteria were pelleted by centrifugation at 6000 X g for 10 min, washed once with sterile saline and resuspended to a final concentration of 1×10^6 CFU/μl (16). Mice were anesthetized using anhydrous ethyl ether and placed beneath a stereoscopic microscope (x40 magnification). The left cornea was wounded by making three 1-mm incisions with a sterile $25^{5/8}$-gauge needle. A 5 μl aliquot of the 10^6 bacterial suspension was topically applied to the wounded corneal surface.

Ocular response to bacterial infection

Corneal disease was scored using a grading scale (17): 0, clear or slight opacity, partially or fully covering the pupil; +1, slight opacity, fully covering the anterior segment; +2, dense opacity, partially or fully covering the pupil; +3, dense opacity, covering the entire anterior segment; and +4, corneal perforation or phthisis. A clinical score was recorded at 1, 3, 5 and /or 7 days postinfection (p.i.) for each mouse for statistical comparison of disease severity. Photographs taken with a slit lamp at 5 or 7 days p.i. illustrated and confirmed the disease score.

VIP treatment

Treatment with VIP has been described before (10). Briefly, C57BL/6 mice received daily intraperitoneal (i.p.) injections of VIP (5 nmol in 100 μl PBS) (Bachem, Torrance, CA) starting 1 day before infection, and, including the day of infection, through 5 days p.i. Control mice were similarly injected with sterile PBS.

siHMGB1 treatment

Use of small interfering RNA (siRNA) *in vivo* has been described previously (18). In these studies, siRNA targeting HMGB1 or siRNA for a non-targeting scrambled sequence (negative control) (Santa Cruz Biotechnology, Santa Cruz, CA) was injected subconjunctivally (5 μl/mouse, 8 μM concentration) into the left eye of C57BL/6 mice on the day before infection, then applied topically onto infected corneas (5 μl/mouse, 4 μM) once on the day of infection and twice on 1 day p.i. The efficacy and specificity of silencing HMGB1 was tested by real time RT-PCR. The siRNAs used in this study were shorter than 21 nucleotides in length to avoid nonspecific siRNA suppression effects via cell surface TLR3 (19).

HMGB1 antibody neutralization

C57BL/6 mice were injected subconjunctivally with 5 μg/mouse anti-HMGB1 antibody (IBL International, Toronto, ON) or control chicken IgY (Jackson ImmunoResearch, West Grove, PA) 1 day before infection, essentially as described before (8). On days 1 and 3 p.i.,

each mouse was injected i.p. with an additional 150 μg (in 150 μl) of anti-HMGB1 antibody. Control mice were similarly injected with chicken IgY. Corneas were harvested 5 days p.i for MPO assay.

Recombinant HMGB1 treatment

Resistant BALB/c mice were treated with recombinant (r) HMGB1 (R&D Systems, Minneapolis, MN). Mice were injected subconjunctivally with 1 μg/5 μl rHMGB1 one day before infection. Control mice received a similar injection of PBS. An additional 1 μg rHMGB1 (in 100 μl) was administered i.p. on days 1 and 3 p.i. with control mice receiving PBS similarly. Corneas were harvested 7 days p.i. for MPO assay.

TLR PCR array

The corneas of VIP and PBS treated C57BL/6 mice were harvested at 3 days p.i. and mRNA prepared and pooled before production of cDNA using an RT^2 First Strand Kit (Qiagen Inc., Valencia, CA). The mRNA levels of 84 TLR related genes were profiled using a Mouse TLR RT^2 Profiler™ PCR Array (Qiagen Inc). HMGB1 levels were further tested by real time RT-PCR and ELISA assays.

Real time RT-PCR

Normal and infected corneas from C57BL/6 mice after VIP or PBS treatment (1, 3, 5, and 7 days p.i.), and after siHMGB1 or control siRNA treatment (1, 3, and 5 days p.i.) were removed after sacrificing mice. Individual corneas were briefly stored in RNA STAT-60™ (Tel-Test, Friendswood, TX) at −20°C before processing. Total corneal RNA was extracted with chloroform (200 μl/ml RNA STAT-60™; Sigma-Aldrich, St Louis, MO), precipitated overnight with isopropanol (500 μl/ml RNA STAT-60™; Sigma-Aldrich) and washed in cold 75% ethanol. To produce a cDNA template for the PCR reaction, 1 μg of each RNA sample was reverse transcribed using Moloney-murine leukemia virus (M-MLV, Invitrogen, Carlsbad, CA). The 20 μl mixture contained 2000U M-MLV-reverse transcriptase, 10U of RNase inhibitor, 500 ng oligo (dT) primers 10mM dNTPs, 100mM DTT, and M-MLV reaction buffer (all from Invitrogen). cDNA products were diluted 1:25 with diethylpyrocarbonate-treated water and a 2 μl cDNA aliquot was used for real-time RT-PCR. mRNA levels of HMGB1, IL-1β, MIP-2, TNF-α, TLR4, RAGE, single Ig IL-1-related receptor (SIGIRR), interleukin 1 receptor-like 1 (ST2), CXCL12, and CXCR4 were tested by real-time RT-PCR (CFX Connect™ Real-Time PCR Detection System; Bio-Rad, Richmond, CA). Real-Time SYBR® Green/Fluorescein PCR Master Mix (Bio-Rad) was used for the PCR reaction with primer concentrations of 10 μM. After a pre-programmed hot start cycle (3 min at 95°C), the parameters used for PCR amplification were: 15s at 95°C and 60s at 60°C with the cycles repeated 45 times. Optimal conditions for PCR amplification of cDNA were established by routine methods (20). The fold differences in gene expression were calculated after normalization to β-actin and are expressed as the relative mRNA concentration ± the standard error of the mean (SEM). Table 1 shows the primer pair sequences used for real-time RT-PCR.

Immunohistochemistry

After VIP treatment, corneal expression of HMGB1 was evaluated using immunohistochemistry and confocal microscopy. Whole eyes were enucleated at 1 and/or 5 days p.i. after VIP (or PBS) treatment, immersed in PBS, embedded in Optimal Cutting Temperature (OCT) medium (Sakura Finetek, Torrance, CA) and frozen in liquid nitrogen. Frozen sections were cut (10 μm thick), and mounted to poly-l-lysine coated glass slides. Slides were incubated overnight at 37°C and fixed in acetone. Sections were incubated 30 min with a blocking reagent (0.01M phosphate buffer containing 2.5% BSA and 1:100 donkey IgG (Jackson ImmunoResearch) at room temperature. Sections were incubated for 1 h in primary antibody, rabbit anti-HMGB1 (1:100; Cell Signaling, Danvers, MA) diluted in blocking agent and then a 1 h incubation in Alexafluor 546 conjugated donkey anti-rabbit (diluted 1:1500 in 0.01M Tris-HCl; Molecular Probes, Eugene, OR). Sections were then incubated for 2 min with SYTOX Green nucleic acid stain (1:20,000-Lonza, Walkersville, MD) and cover slipped using Vectashield mountant (Vector Laboratories, Burlingame, CA). Negative controls were similarly treated with species specific IgG, replacing the primary antibody. Sections were observed and digital images captured with a confocal microscope (TCS SP2; Leica Microsystems, Exton, PA).

To determine if macrophages and/or PMN are a source of HMGB1, infected corneas from C57BL/6 mice were harvested 3 days p.i. embedded, sectioned, and incubated in blocking reagent as described above. Sections were incubated simultaneously with two primary antibodies, rabbit anti-HMGB1 and either rat anti-macrophage (F4/80-Santa Cruz), or rat anti-neutrophil (NIMP-R14, Abcam, Cambridge, MA) all at 1:100, diluted in blocking agent for 1 h followed by a 1 h incubation in Alexafluor 647 conjugated donkey anti-rabbit and Alexafluor 546 conjugated donkey anti-rat (both diluted 1:1500 in 0.01M Tris-HCl, Molecular Probes). Sections were then incubated with SYTOX Green nucleic acid stain and cover slipped using Vectashield mountant as described above. Negative controls were similarly treated with species specific IgG, to replace primary antibodies. Sections were observed and digital images captured with a confocal microscope (TCS SP8; Leica Microsystems).

ELISA

Individual corneas taken for ELISA were homogenized in 500 μl PBS with 0.1% Tween 20 with a protease inhibitor cocktail (Roche Diagnostics, Indianapolis, IN) and centrifuged at 12,000 X *g* for 5 min. After VIP/PBS or siHMGB1/scrambled siRNA treatment, normal (uninfected) and infected samples were harvested and prepared as described above at 1or 3 and 5 days p.i. A 50 μl aliquot of each supernatant was assayed in duplicate for HMGB1 protein per the manufacturer's instructions (Chondrex, Inc. Redmond, WA). Sensitivity of the assay was 1.6 ng/ml. After siHMGB1 or scrambled siRNA treatment, normal (uninfected) and infected samples were harvested and prepared as described above at 3 and 5 days p.i. A 50 μl aliquot of each supernatant was assayed in duplicate for IL-1β, MIP-2, and CXCL12 protein (R&D Systems) and 100 μl was assayed in duplicate for CXCR4 protein (My BioSource, San Diego, CA) per the manufacturer's instructions. After siHMGB1 or scrambled siRNA treatment and infection with clinical isolate KEI 1025, corneas were harvested at 3 and 5 days p.i. and assayed for IL-1β and MIP-2 protein.

Sensitivities of the assays were 2.31 pg/ml (IL-1β), 1.5 pg/ml (MIP-2), 44 pg/ml (CXCL12), and 75 pg/ml (CXCR4).

Myeloperoxidase (MPO) assay

An MPO assay was used to quantitate PMN number in the cornea of siHMGB1 vs scrambled controls (infected with strain 19660 and/or KEI 1025 clinical isolate), anti-HMGB1 vs IgY, and rHMGB1 vs PBS. Individual corneas were removed at 3 and/or 5 days p.i. and homogenized in 1.0 ml of 50mM phosphate buffer (pH 6.0) containing 0.5% hexadecyltrimethyl-ammonium (Sigma). Samples were freeze-thawed four times and after centrifugation, 100 μl of the supernatant was added to 2.9 ml of 50 mM phosphate buffer containing *o*-dianisidine dihydrochloride (16.7 mg/ml, Sigma) and hydrogen peroxide (0.0005%). The change in absorbency at 460 nm was monitored for 5 min at 30 sec intervals. The slope of the line was determined for each sample and used to calculate units of MPO/cornea. One unit of MPO activity is equivalent to ~2×10^5 PMN (21).

Staining and quantitation of monocytes and macrophages from the infected cornea

After siHMGB1 or scrambled control treatment, individual corneas were harvested at 3 and 5 days p.i. and incubated in 1 ml (1 mg/ml) Type I collagenase (Sigma) in HBSS (Invitrogen) containing 5% FBS for 2–2.5 h at 37°C. The samples were pipetted several times every 15 min to aid in dissociation of the cornea. Cell suspensions were centrifuged at 300 x *g*, 4°C for 5 min to pellet cells. Cells in suspension were fixed for 10 min in 100 μl 0.01% formaldehyde/PBS at room temperature. Cells were permeabilized by adding 100 μl of permeabilizing reagent (0.5% Tween 20/PBS) and incubated for an additional 15 min. Cells were centrifuged and the cell pellet washed with 500 μl permeabilizing reagent. The cell suspensions were incubated separately with 100 μl rat anti-monocyte and macrophage antibody (MOMA-2, Abcam) diluted 1:25, or rat anti-macrophage (F4/80, Santa Cruz) diluted to 50 μg/ml in permeabilization reagent for 1 h on ice. After washing in 500 μl PBS with 5% FBS, the cell suspension was incubated in 100 μl FITC-conjugated donkey anti-rat IgG (H+L) (Jackson ImmunoResearch) diluted 1:50 in permeabilization buffer for 1 h on ice. Cells were washed with 500 μl PBS with 5% FBS and positive cells counted on a Cellometer Vision (Nexcelom Biosciences, Lawrence, MA) and expressed as a percentage of the total cell number. The cells also were analyzed using the Cellometer software package (FCS Express 4) and data expressed as dot plots. Cell viability following staining and quantitation was >85%.

Statistical analysis

The difference in clinical score between two groups at each time was tested by the Mann-Whitney U test; horizontal bar indicates median value. An unpaired, two-tailed Student's t-test was used to determine the statistical significance of the real-time RT-PCR, ELISA, MPO and cell count data, and considered significant at $p \leq 0.05$. All these experiments were repeated once to ensure reproducibility and data are shown as mean ± standard error of the mean (SEM).

Results

HMGB1 in cornea

PCR array revealed that VIP treatment down-regulated mRNA expression of HMGB1 in C57BL/6 cornea 13.72 fold over PBS treatment at 3 days p.i. (Fig. 1A). The kinetics of down-regulation was tested by real time RT-PCR and ELISA and the data are shown in Fig. 1B and C. Although HMGB1 mRNA was similarly expressed in the uninfected, normal cornea of both groups, its expression was decreased after infection. VIP vs PBS treatment significantly reduced HMGB1 at 1, 3, 5, and 7 days p.i. ($p<0.001$ for 1 and 3 days, $p<0.05$ and $p<0.01$, for 5 and 7 days p.i.) when compared to levels after PBS treatment (Fig. 1B). ELISA analysis showed that protein levels of HMGB1 were significantly down-regulated after VIP treatment in the uninfected, normal cornea and at 3 and 5 days p.i. ($p<0.01$, $p<0.001$ and $p<0.001$) when compared to levels in PBS treated mice (Fig. 1C).

HMGB1 staining after VIP treatment

Immunohistochemistry was used to localize the expression of HMGB1 in the infected cornea at 1 and 5 days p.i. after treatment with VIP or PBS. At 1 day p.i., staining for HMGB1 (red) was seen in both the corneal epithelium (Epi, arrows) and stroma (Stroma, arrows) after PBS treatment (Fig. 2A), but was observed only in the epithelium (Epi, arrows) after VIP treatment (Fig. 2B). At 5 days p.i., staining for HMGB1 was seen in the corneal stroma (Stroma, arrows) of PBS treated mice (Fig. 2C); VIP treated mice (Fig. 2D) had much reduced corneal staining and appeared more similar to negative controls (Fig. 2E and F).

RNA interference

HMGB1 knockdown was used to test effects on disease pathogenesis and data are shown (Fig. 3A–C). Significantly lower disease scores were seen at 3 and 5 days p.i. in the siHMGB1 vs scrambled, control treated mice ($p=0.05$ and $p=0.01$, respectively). However, no significant difference in disease response was observed between groups at 1 day p.i. Photographs taken with a slit lamp documented corneal disease in siHMGB1 (Fig. 3B, +2 to +3) vs scrambled control (Fig. 3C, +4) treated mice at 5 days p.i. To confirm the specificity of HMGB1 knockdown, mRNA levels were tested and showed (Fig. 3D) that silencing HMGB1 was significant and specific up to 5 days p.i. ($p<0.001$). Protein levels also were tested (Fig. 3E) and after silencing were significantly reduced at 1 and 5 days p.i. ($p=0.003$ and $p=0.03$). To test the cell source of HMGB1 after infection, dual immunostaining was used and showed (magenta) that some, but not all stromal macrophages (Fig. 3F) and/or PMN (Fig. 3G) stained specifically for HMGB1. Controls (Fig. 3H and I) showed no specific immunostaining for macrophages (H) or PMN (I).

Real time RT-PCR

IL-1β (Fig. 4A), MIP-2 (Fig. 4B), TNF-α (Fig. 4C), TLR4 (Fig. 4D), and RAGE (Fig. 4E) mRNA levels were tested and each was significantly reduced at 5 days p.i. in siHMGB1 vs scrambled control treated animals ($p<0.001$ for all except RAGE, $p<0.01$). mRNA levels of anti-inflammatory molecules SIGIRR (Fig. 4F) and ST2 (Fig. 4G) were slightly but

significantly elevated at 5 days p.i. in siHMGB1 vs scrambled control treated corneas ($p<0.01$ and 0.05). No differences were detected between groups in the uninfected, contralateral normal cornea for any of the genes tested (Fig. 4A–G).

ELISA and MPO after RNA interference

ELISA assays were used to confirm the reduction in selected molecules at the protein level. IL-1β was significantly reduced at 5 days p.i. in siHMGB1 compared to scrambled control treated mice ($p<0.01$) with no difference between groups in uninfected, normal corneas or at 3 days p.i. (Fig. 5A). MIP-2 protein, a chemoattractant for PMN, was significantly lowered in siHMGB1 vs scrambled control treated mice at both 3 and 5 days p.i. ($p<0.01$ and $p=0.05$) with no significant difference between groups in uninfected, normal control corneas of either group (Fig. 5B). Since silencing HMGB1 reduced levels of both IL-1β and MIP-2, an MPO assay was used to quantitate the number of PMN in the infected cornea following siHMGB1 vs scrambled control treatment (Fig. 5C). MPO showed a significant reduction in PMN at 5 days p.i. in siHMGB1 vs scrambled control treated mice ($p=0.02$); no difference was detected between groups at 3 days p.i.

RT-PCR, ELISA and monocyte/macrophage cell count

To explore HMGB1 signaling pathway involvement, real time RT-PCR analysis tested mRNA expression of CXCL12 in siHMGB1 treated mouse cornea compared to scrambled controls. Levels were significantly reduced at 1 day p.i. ($p<0.001$), but no difference was seen between groups in uninfected normal cornea, or at 3 and 5 days p.i. (Fig. 6A). ELISA assay (Fig. 6B) showed that protein expression of CXCL12 was reduced significantly in the normal cornea ($p<0.04$) and after 5 days p.i. ($p<0.001$). Silencing HMGB1 also significantly reduced expression of CXCR4 mRNA in the cornea at 1, 3, and 5 days p.i. compared to the scrambled control ($p<0.001$, 0.01 and 0.01), with no difference between groups in the uninfected, normal control (Fig. 6C). CXCR4 protein in the cornea was significantly reduced after silencing HMGB1 at 5 days p.i ($p<0.01$) compared to scrambled control treatment. No difference was detected between groups in uninfected, normal cornea or at 3 days p.i. (Fig. 6D). The number of monocytes and macrophages were quantitated separately after infection and corneal disaggregation to determine if siHMGB1 diminished HMGB1 dependent mononuclear cell recruitment (Fig. 7A–E). At 3 days p.i., no difference was seen in either monocyte/macrophage (MOMA positive) or macrophage (F4/80 positive) cells as a percent of total corneal cells. However, at 5 days p.i., both populations of cells were significantly reduced ($p=0.04$ and $p=0.007$) when compared with scrambled control treated values (Fig. 7A). Dot plots are also provided and show fluorescence intensity and cell size for the 3 and 5 day p.i. time points. At 3 days, no difference was seen between groups for MOMA positive (intermediate and large cells) or F4/80 positive (large) cells (Fig. 7B and C). However, at 5 days p.i., siHMGB1 treatment reduced the proportion of intermediate and large size cell size populations when compared with scrambled control treatment (Fig.7D and E).

Antibody neutralization, rHMGB1 and clinical isolate testing

To confirm the siRNA data selected studies were performed. In the first, neutralizing antibody to HMGB1 was tested and showed that antibody treatment improved clinical score

at 5 days p.i. (Fig. 8A) and slit lamp confirmed the perforation response typical of the control treated group (Fig. 8C) compared with a +3 opacity, a typical response score in the antibody treated mice (Fig. 8B). MPO assay confirmed that less opacity was consistent with a decrease in PMN in the antibody vs IgY treated control mice at 5 days p.i. (Fig. 8D). Resistant BALB/c mice were treated with rHMGB1 and clinical score was assessed and found significantly reduced in the PBS vs rHMGB1 treated mice at both 5 and 7 days after infection (Fig. 9A, $p=0.02$ and $p=0.005$). The response at 7 days in the controls (Fig. 9C) shows an almost clear cornea, when compared with a +1 to +2 in the recombinant treated (Fig. 9B) mice. MPO assay also was done and rHMGB1 mice had a greater number of PMN in cornea vs PBS controls (Fig. 9D, $p<0.05$) at 7 days p.i.) A clinical isolate KEI 1025 also was tested after siRNA HMGB1 treatment of C57BL/6 mice and the data shown in Fig. 10 (A–F). Clinical score (Fig. 10A) was reduced after silencing at 3 and 5 days p.i. ($p<0.01$ for both). Corneal opacity in HMGB1 knockdown mice was reduced to +1 (Fig. 10B), while controls (Fig. 10C) exhibited a +2 to +3 response indicative of increased disease; a ring infiltrate was also visible in the corneal periphery. Protein levels for IL-1β, and MIP-2 were tested (Fig. 10D and E) and silencing reduced each of the cytokines significantly at 5 ($p<0.001$, $p<0.0001$) but not 3 days p.i. MPO (Fig. 10F) revealed reduced PMN in cornea at both 3 and 5 days p.i. ($p<0.05$, $p<0.001$).

Discussion

VIP is a short-lived small peptide hormone that is produced by the gut, pancreas and brain. It has enjoyed intense interest for treating inflammatory diseases clinically, but some issues remain (22). One of them, its delivery, is critical to the therapeutic use of VIP in human disease. In this regard, VIP is degraded quickly by enzymes, catalytic antibodies, and spontaneous hydrolysis in biological fluids (13). Furthermore, systemic administration of VIP has been shown to cause cardiovascular side effects (23). Nonetheless, VIP given experimentally reduces the incidence of perforation in the *P. aeruginosa* infected mouse cornea and VIP knockout mice are highly susceptible to infection with accelerated time to perforation when compared with wild type controls (24). VIP is in general, anti-inflammatory, in that it protects against several immune disorders by regulating a wide panel of inflammatory mediators. VIP reduces sepsis lethality induced by cecal ligation and puncture and/or or by injection of live *Escherichia coli* (25). Of interest to us, was the fact that the therapeutic effect of VIP was accompanied by a decrease in systemic levels of the alarmin, HMGB1 (12). In addition, administration of recombinant HMGB1 was shown to completely reverse the protective effect of VIP in experimental sepsis (12). HMGB1, originally described as a nuclear protein that bends DNA (25) is therefore a molecular target that provides a wide window for clinical intervention in diseases such as sepsis, and potentially other infectious diseases such as bacterial keratitis. *In vitro* and *ex vivo* (12) studies show that VIP down-regulates translocation of HMGB1 from the nucleus to the cytoplasm and its subsequent secretion (26) by activated macrophages, suggesting that macrophages are major targets in the inhibitory activity of this neuropeptide. In other studies, (27, 28) administration of anti-HMGB1 antibodies or inhibitors rescued mice from lethal experimental sepsis, even when the first dose was given 24 h after onset. Taken together, these data establish HMGB1 as a late mediator of experimental sepsis with a wider

therapeutic window than early mediators such as TNF (27). In the keratitis model used herein, VIP treatment also reduced HMGB1 in the infected cornea over 13 fold and RT-PCR confirmed its reduction at the mRNA level and revealed the kinetics of the response. HMGB1 mRNA levels were reduced as early as 1 day after infection, but reduction persisted throughout 7 days p.i. of observation, consistent with the observation in sepsis of its late persistence, allowing it as a potential target in patients. Protein levels were reduced at all times tested as well. Immunostaining revealed that the effects of VIP treatment decreased HMGB1 staining in both the epithelium and stroma (infiltrated with PMN and macrophages), at both 1 and 5 days p.i. when compared with PBS treatment. Using this technique, we also found that both (but not all) PMN and macrophages secrete HMGB1 in the infected cornea.

Unlike IL-1β (8), the role for HMGB1 in bacterial disease is less clear (29). Although HMGB1 is a mediator of late-phase endotoxic shock and neutralizing antibodies are protective (25), conditional deletion of HMGB1 from myeloid cells resulted in increased sensitivity to endotoxic shock (30). Conditional knockout of HMGB1 from myeloid cells made mice more susceptible to *L. monocytogenes* infections (30). However, neutralizing antibodies against HMGB1 in cystic fibrosis patients protected against *P. aeruginosa* infection by reducing lung injury, bacterial load and PMN persistence (31). This suggests a similarity to the negative role of excessive IL-1β in *P. aeruginosa* corneal infections (8). HMGB1 is released following necrosis of cells or during inflammasome activation after bacterial infection. Since HMGB1 can also bind to a wide variety of bacterial products (32), it is likely that HMGB1 can also potentiate the immune sensing of several bacterial pathogens associated molecular patterns (PAMPs).

Therefore, to further test the effect of reducing levels of HMGB1 on bacterial keratitis, knockdown of HMGB1 was used and confirmed the importance of the molecule in infected corneas. This was evidenced by observation that scrambled control treated vs siHMGB1 mice had perforated corneas (7/10) when compared to knockdown (1/10) treatment. Silencing HMGB1 also reduced both mRNA and protein levels of the alarmin as well as several pro-inflammatory cytokines at the mRNA level, including IL-1β, MIP-2, TNF-α, TLR4 and RAGE. Protein levels of both IL-1β and MIP-2, as well as MPO levels also were decreased, similar to the affects reported by others (31) using antibody neutralization of HMGB1 in a mouse model of cystic fibrosis. In contrast, anti-inflammatory molecules SIGIRR and ST2 were increased, which could participate to favorably affect the overall disease response.

Accumulating evidence indicates that HMGB1 also can stimulate migration of monocytes (33), dendritic cells (34, 35) and neutrophils (36). These raise a possibility that extracellular HMGB1 may recruit cells to sites of infection or injury (37), thereby functioning as a potential chemokine (38). HMGB1-induced cell migration requires activation of the canonical and non-canonical NF-κB pathways, which in turn leads to transcription of the *Cxcl12* gene (39). Elegant recent studies have shown that HMGB1-induced recruitment of inflammatory cells depends on CXCL12 which forms a heterocomplex with HMGB1 and acts exclusively through the α-chemokine receptor, CXCR4 and not through other HMGB1 receptors (40). In those studies, fluorescence resonance energy transfer data showed that the

HMGB1- CXCL12 heterocomplex promotes different conformational rearrangements of CXCR4 from that of CXCL12 alone and is responsible for mononuclear cell migration.

This study (40) prompted us to test whether monocytes and macrophages were directly affected by silencing HMGB1 in the keratitis model. Levels of CXCL12 and CXCR4 at both mRNA and protein levels were examined after silencing and were reduced at various time points following infection. To test if silencing affected monocytic cells, markers for monocytes/macrophages (MOMA) and only macrophages (F4/80) were used separately to label the cells, followed by quantitation. Positive cells for each marker were expressed as a percentage of total corneal infiltrated cells; no difference was observed at 3 days p.i. but by 5 days p.i., silencing had reduced both MOMA (monocytes and macrophages) and F4/80 (macrophages only) positive cells significantly compared with scrambled controls. In other studies, mononuclear cell recruitment *in vivo* into air pouches and injured muscles depended on the heterocomplex formation and furthermore, provided evidence that CXCR4 signaling was inhibited by AMD3100 (40, 41).

In addition to regulation of monocytic populations of cells, in allergic lung inflammation (42) recent data suggest that HMGB1 directs Th17 skewing by regulating dendritic cell function, suggesting that HMGB1 drives the DC-polarized Th17-type response and that blocking HMGB1 may be beneficial in attenuating neutrophilic airway inflammation in asthma via this mechanism. The latter was not investigated in the current study reported herein, but suggests another possible indirect role for HMGB1 in recruitment of PMN during bacterial keratitis.

Other approaches to modulate levels of HMGB1, including antibody neutralization, provided corroborative data that reduction of HMGB1 improved disease outcome (no perforation). This was accompanied by reduced PMN (27, 28) in the cornea which is consistent with, but not as effective as with siRNA treatment. This could reflect that the amount of antibody injected, or the number of injections, were insufficient to provide a greater beneficial affect. However, when we injected resistant mice with rHMGB1 (12), disease worsened considerably and was associated with enhanced PMN in cornea. Lastly, using a clinical isolate KEI 1025, and silencing HMGB1, we found that the disease response was consistent with the siRNA studies using C57BL/6 mice and the ATCC strain 19660. Corneal disease was reduced considerably, and silencing appeared even more efficacious with the clinical isolate than with the ATCC strain, perhaps reflecting differences in virulence between the two. Consistent with reduced disease, IL-1β, and MIP-2 protein, as well as MPO were all reduced significantly after silencing.

Alternatively, HMGB1 has been identified as essential in cardiac repair during murine acute myocardial infarction, resulting in cardiac regeneration via resident c-kit+ (progenitor) cell activation (43). Thus, pharmacological or other types of modulation coupled with antibiotic treatment, rather than abrogation of systemic HMGB1 accumulation, as with knockdown, may provide an alternate approach to explore further for treatment of bacterial keratitis.

Acknowledgments

Grant Support: NEI/NIH grants R01EY016058, R01EY002986, P30EY004068 and by Research to Prevent Blindness (unrestricted grant to the Department of Ophthalmology/Kresge Eye Institute).

References

1. Wilhelmus KR. Review of clinical experience with microbial keratitis associated with contact lenses. CLAO J. 1987; 13:211–214. [PubMed: 3331130]
2. Hazlett LD. Corneal response to *Pseudomonas aeruginosa* infection. Prog. Retin. Eye Res. 2004; 23:1–30. [PubMed: 14766315]
3. Moon MM, Hazlett LD, Hancock RE, Berk RS, Barrett RP. Monoclonal antibodies provide protection against ocular *Pseudomonas aeruginosa* infection. Invest. Ophthalmol. Vis. Sci. 1988; 29:1277–1284. [PubMed: 2843483]
4. Steuhl K-P, Doring G, Henni A, Thiel H-J, Botzenhart K. Relevance of host-derived and bacterial factors in *Pseudomonas aeruginosa* corneal infection. Infect. Immun. 1987; 28:1559–1568.
5. Thiel H-J, Steul K-P, Doring G. Therapy of *Pseudomonas aeruginosa* eye infections. Antbiot. Chemother. 1987; 39:92–101.
6. Hazlett LD, Rosen DD, Berk RS. Experimental *Pseudomonas* keratitis in immunosuppressed hybrid mice. Ophthalmic Res. 1977; 9:374–380.
7. Chusid MJ, Davis SD. Experimental bacterial keratitis in neutropenic guinea pigs: polymorphonuclear leukocytes in corneal host defense. Infect. Immun. 1979; 24:948–952. [PubMed: 112062]
8. Rudner XL, Kernacki KA, Barrett RP, Hazlett LD. Prolonged elevation of IL-1 in *Pseudomonas aeruginosa* ocular infection regulates macrophage-inflammatory protein-2 production, polymorphonuclear neutrophil persistence, and corneal perforation. J. Immunol. 2000; 164:6576–6582. [PubMed: 10843717]
9. Kernacki KA, Barrett RP, Hobden JA, Hazlett LD. Macrophage inflammatory protein-2 is a mediator of polymorphonuclear neutrophil influx in ocular bacterial infection. J. Immunol. 2000; 164:1037–1045. [PubMed: 10623854]
10. Szliter EA, Lighvani S, Barrett RP, Hazlett LD. Vasoactive intestinal peptide balances pro- and anti-inflammatory cytokines in the *Pseudomonas aeruginosa*-infected cornea and protects against corneal perforation. J. Immunol. 2007; 178:1105–1114. [PubMed: 17202374]
11. Jiang X, McClellan SA, Barrett RP, Zhang Y, Hazlett LD. Vasoactive intestinal peptide downregulates proinflammatory TLRs while upregulating anti-inflammatory TLRs in the infected cornea. J. Immunol. 2012; 189:269–278. [PubMed: 22661083]
12. Chorny A, Delgado M. Neuropeptides rescue mice from lethal sepsis by down-regulating secretion of the late-acting inflammatory mediator high mobility group box 1. Am. J. Pathol. 2008; 172:1297–1302. [PubMed: 18385521]
13. Wu D, Lee D, Sung YK. Prospect of vasoactive intestinal peptide therapy for COPD/PAH and asthma: a review. Respiratory Res. 2011; 12:45. http://respiratory-research.com/content/12/1/4.
14. Yang H, Ochani M, Li J, Qiang X, Tanovic M, Harris HE, Susarla SM, Luis U, Wang H, DiRaimo R, Czura CJ, Wang H, Roth J, Warren HS, Fink MP, Fenton MJ, Andersson U, Tracey KJ. Reversing established sepsis with antagonists of endogenous high-mobility group box 1. Proc. Natl. Acad. Sci. USA. 2004; 101:296–301. [PubMed: 14695889]
15. Liu K, Mori S, Takabashi HK, Tomono Y, Wake H, Kanke T, Sato Y, Hiraga N, Adachi N, Yoshino T, Nishibori M. Anti-high mobility group box 1 monoclonal antibody ameliorates brain infarction induced by transient ischemia in rats. FASEB J. 2007; 21:3904–3916. [PubMed: 17628015]
16. Kwon B, Hazlett LD. Association of CD4+ T cells-dependent keratitis with genetic susceptibility to *Pseudomonas aeruginosa* . J. Immunol. 1997; 159:6283–6290. [PubMed: 9550433]
17. Hazlett LD, Moon MM, Strejc M, Berk RS. Evidence for *N*-acetylmannosamine as an ocular receptor for *P. aeruginosa* adherence to scarified cornea. Invest. Ophthalmol. Vis. Sci. 1987; 28:1978–1985. [PubMed: 3119512]

18. Huang X, Barrett RP, McClellan SA, Hazlett LD. Silencing Toll-like receptor-9 in *Pseudomonas aeruginosa* keratitis. Invest. Ophthalmol. Vis. Sci. 2005; 46:4209–4216. [PubMed: 16249500]
19. Kleinman ME, Yamada K, Takeda A, Chandrasekaran V, Nozaki M, Baffi JZ, Albuquerque RJ, Yamasaki S, Itaya M, Pan Y, Appukuttan B, Gibbs D, Yang Z, Karikó K, Ambati BK, Wilgus TA, DiPietro LA, Sakurai E, Zhang K, Smith JR, Taylor EW, Ambati J. Sequence- and target-independent angiogenesis suppression by siRNA via TLR3. Nature. 2008; 452:591–597. [PubMed: 18368052]
20. Heid CA, Stevens J, Livak KJ, Williams PM. Real time quantitative PCR. Genome Res. 1996; 6:986–994. [PubMed: 8908518]
21. Williams RN, Paterson CA, Eakins KE, Bhattacherjee P. Quantification of ocular inflammation: evaluation of polymorphonuclear leucocyte infiltration by measuring myeloperoxidase activity. Curr. Eye Res. 1982; 2:465–470. [PubMed: 6303695]
22. Wang H, Zhu S, Zhou R, Lei W, Sama AE. Therapeutic potential of HMGB1-targeting agents in sepsis. Expert Rev. Mol. Med. 2008 Nov.10:e32. 2008. [PubMed: 18980707]
23. Morice A, Unwin RJ, Sever PS. Vasoactive intestinal peptide causes bronchodilation and protects against histamine-induced bronchoconstriction in asthmatic subjects. Lancet. 1983; 2:1225–1227. [PubMed: 6139572]
24. Jiang X, McClellan SA, Barrett RP, Zhang Y, Foldenauer ME, Hazlett LD. The role of VIP in cornea. Invest. Ophthalmol. Vis. Sci. 2012; 53:7560–7566. [PubMed: 23074208]
25. Wang H, Bloom O, Zhang M, Vishnubhakat JM, Ombrellino M, Che J, Frazier A, Yang H, Ivanova S, Borovikova L, Manogue KR, Faist E, Abraham E, Andersson J, Andersson U, Molina PE, Abumrad NN, Sama A, Tracey KJ. HMG-1 as a late mediator of endotoxin lethality in mice. Science. 1999; 285:248–251. [PubMed: 10398600]
26. Gardella S, Andrei C, Ferrera D, Lotti LV, Torrisi MR, Bianchi ME, Rubartelli A. The nuclear protein HMGB1 is secreted by monocytes via a non-classical, vesicle-mediated secretory pathway. EMBO Rep. 2002; 3:995–1001. [PubMed: 12231511]
27. Andersson U, Tracey KJ. HMGB1 is a therapeutic target for sterile inflammation and infection. Annu. Rev. Immunol. 2011; 29:139–162. [PubMed: 21219181]
28. Qin S, Wang H, Yuan R, Li H, Ochani M, Ochani K, Rosas-Ballina M, Czura CJ, Huston JM, Miller E, Lin X, Sherrry B, Kumar A, LaRosa G, Newman W, Tracey KJ, Yang H. Role of HMGB1 in apoptosis-mediated sepsis lethality. J. Exp. Med. 2006; 203:1637–1642. [PubMed: 16818669]
29. Keyel, PA. How is inflammation initiated? Individual influences of IL-1, IL-18 and HMGB1. Cytokine. 2014. http;//dx.doi.org/10.1016/jcyto2014.03.007
30. Yanai H, Matsuda H, An J, Koshiba R, Mishio J, Negishi H, Ikushima H, Onoe T, Ohdan H, Yoshida N, Taniguchi T. Conditional ablation of HMGB1 in mice reveals its protective function against endotoxemia and bacterial infection. Proc. Natl. Acad. Sci. USA. 2013; 110:20699–20704. [PubMed: 24302768]
31. Entezari M, Weiss DJ, Sitapara R, Whittaker L, Wargo MJ, Li J, Wang H, Sharma L, Phan BD, Javdan M, Chavan SS, Miller EJ, Tracey KJ, Mantell LL. Inhibition of high-mobility group box 1 protein (HMGB1) enhances bacterial clearance and protects against *Pseudomonas aeruginosa* pneumonia in cystic fibrosis. Mol. Med. 2012; 18:477–485. [PubMed: 22314397]
32. Bianchi ME. HMGB1 loves company. J. Leukoc. Biol. 2009; 86:573–576. [PubMed: 19414536]
33. Rouhianen A, Kuja-Panula J, Wilkman E, Pakkanen J, Stenfors J, Tuominen RK, Lepäntalo M, Carpén O, Parkkinen J, Rauvala H. Regulation of monocyte migration by amphoterin (HMGB1). Blood. 2004; 104:1174–1182. [PubMed: 15130941]
34. Yang D, Cheng Q, Yang H, Tracey KJ, Bustin M, Oppenheim JJ. High mobility group box-1 protein induces the migration and activation of human dendritic cells and acts as an alarmin. J. Leukoc. Biol. 2007; 81:59–66. [PubMed: 16966386]
35. Dumitriu IE, Bianchi ME, Bacci M, Menfredi AA, Rovere-Querini P. The secretion of HMGB1 is required for the migration of maturing dendritic cells. J. Leukoc. Biol. 2007; 81:84–91. [PubMed: 17035340]

36. Orlova VV, Choi EY, Xie C, Chavakis E, Bierhaus A, Ihanus E, Ballantyne CM, Gahmberg CG, Bianchi ME, Nawroth PP, Chavakis T. A novel pathway of HMGB1-mediated inflammatory cell recruitment that requires Mac-1-integrin. EMBO J. 2007; 26:1129–1139. [PubMed: 17268551]

37. Degryse B, Bonaldi T, Scaffidi P, Muller S, Resnati M, Sanvito F, Arrigoni G, Bianchi ME. The high mobility group (HMG) boxes of the nuclear protein HMGB1 induce chemotaxis and cytoskeleton reorganization in rat smooth muscle cells. J. Cell Biol. 2001; 152:1197–1206. [PubMed: 11257120]

38. Degryse B, Virgilian M. The nuclear protein HMGB1, a new kind of chemokine? FEBS Lett. 2003; 553:11–17. [PubMed: 14550538]

39. Penzo M, Molteni R, Suda T, Samaniego S, Raucci A, Habiel DM, Miller F, Jiang HP, Li J, Pardi R, Palumbo R, Olovotto E, Kew RR, Bianchi ME, Marcu KB. Inhibitor of NF-kappa B kinases alpha and beta are both essential for high mobility group box 1-mediated chemotaxis. J. Immunol. 2010; 184:4497–4509. [PubMed: 20231695]

40. Schiraldi M, Raucci A, Muñoz LM, Livoti E, Celona B, Venereau E, Apuzzo T, DeMarchis F, Pedotti M, Bachi A, Thelen M, Varani L, Mellado M, Proudfoot A, Bianchi ME, Uguccioni M. HMGB1 promotes recruitment of inflammatory cells to damaged tissues by forming a complex with CXCL12 and signaling via CXCR4. J. Exp. Med. 2012; 209(3):551–563. [PubMed: 22370717]

41. Hendrix CW, Collier A, Lederman M, Schols D, Pollard RB, Richard B, Brown S, Brooks JJ, Coombs R, Glesby M, Flexner C, Bridger GJ, Badel K, MacFarland R, Henson WW, Calandra G. Safety, Pharmacokinetics, and antiviral activity of AMD3100, a selective CXCR4 receptor inhibitor, in HIV-1 infection. JAIDS. 2004; 37:1253–1262. [PubMed: 15385732]

42. Zhang F, Huang G, Hu B, Fang LP, Cao EH, Xin XF, Song Y, Shi Y. Anti-HMGB1 neutralizing antibody ameliorates neutrophilic airway inflammation by suppressing dendritic cell-mediated Th17 polarization. Mediators Inflamm. 2014 Epub 2014 May 15.

43. Limana F, Esposito G, Fasanaro P, Foglio E, Arrcelli D, Voellenkle C, DiCarlo A, Avitabile D, Martelli F, Russo MA, Pompilio G, Germani A, Capogtossi MC. Transcriptional profiling of Hmgb1-induced myocardial repair identifies a key role for notch signaling. Mol. Therapy. 2013

A

Gene	Fold downregulation
	VIP-3d /PBS-3d
Hmgb1	-13.72

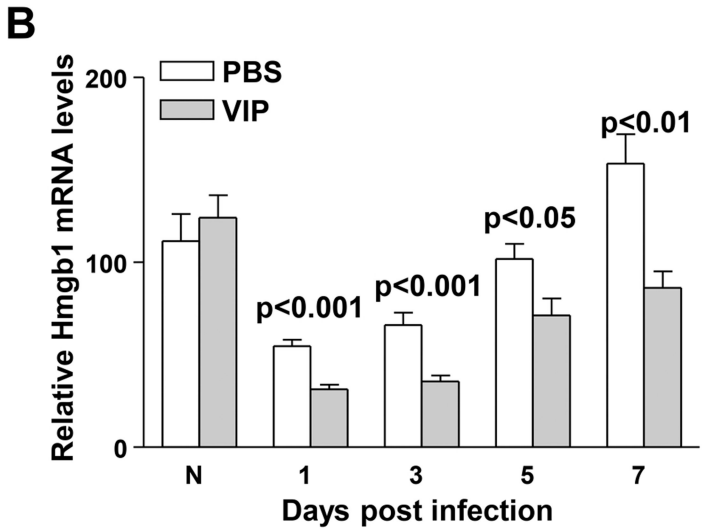

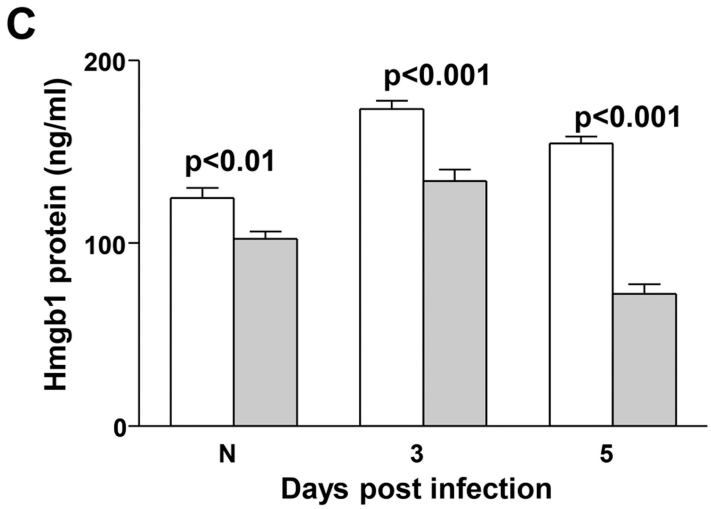

Figure 1. Effect of VIP treatment

PCR array of VIP and PBS treated mouse corneas at 3 days p.i. (n=5/group) showed a 13.72 fold down-regulation of HMGB1 after VIP treatment (**A**). Real time RT-PCR showed significant down-regulation of HMGB1 in VIP treated corneas at 1, 3, 5, and 7 days p.i. ($p<0.001$, $p<0.001$, $p<0.05$ and $p<0.01$), but no difference between normal, uninfected corneas (n=5/group/time) (**B**). ELISA analysis showed significantly less HMGB1 protein in the normal, uninfected corneas of VIP compared to PBS treated mice ($p<0.01$) and at 3 and

5 days p.i. ($p<0.001$ for both) (**C**). (n=5/group/time) Data shown in (**B)** and (**C)** analyzed using a two-tailed Student's t-test and shown as the mean ± SEM.

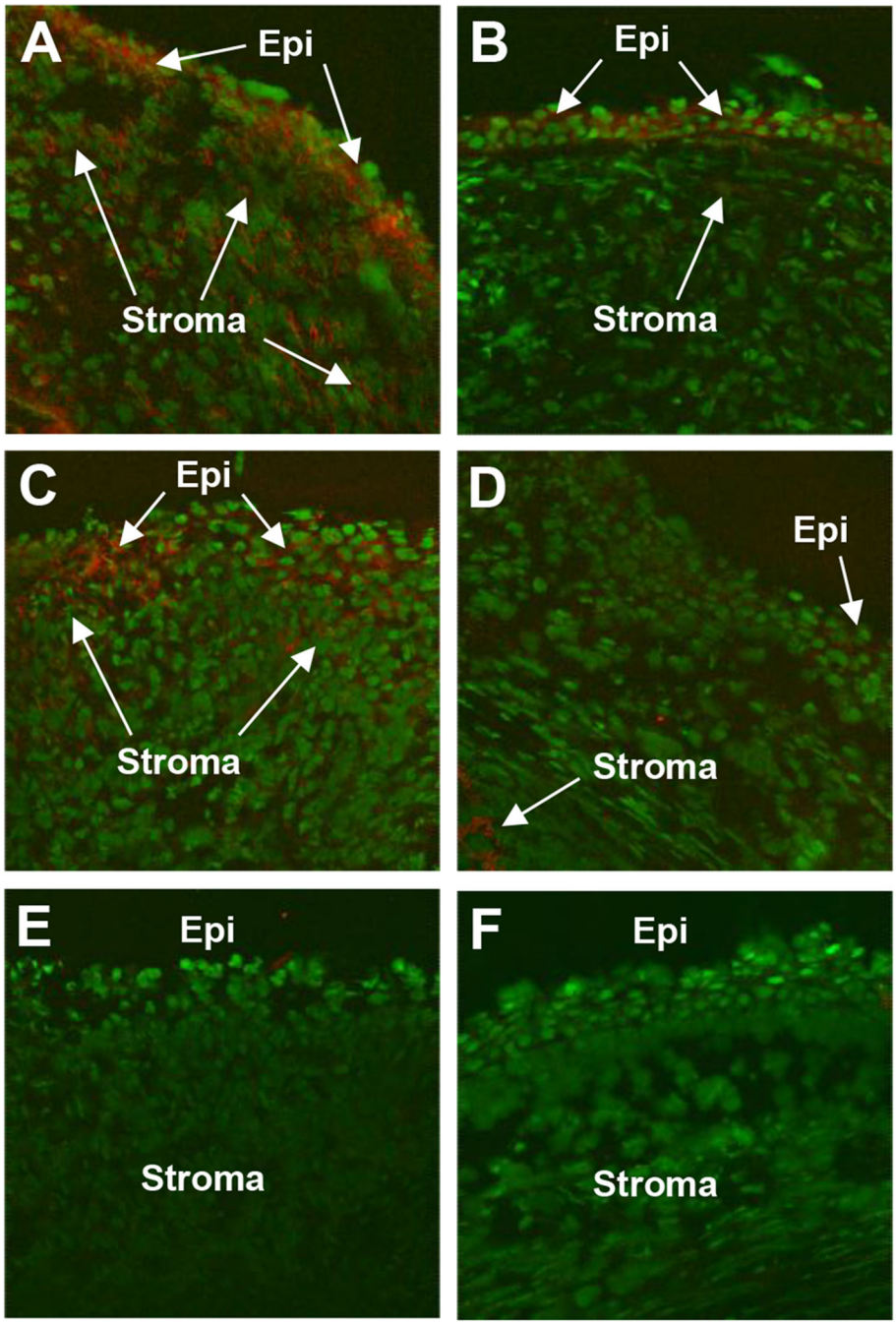

Figure 2. HMGB1 corneal staining after VIP treatment

More positive staining for HMGB1 (red) was seen after PBS (**A**) when compared to VIP treatment (**B**) at 1 day p.i. Staining at 5 days p.i. also showed more corneal HMGB1 (red) in the PBS (**C**) vs VIP treated animals (**D**). Negative controls in which species specific IgG replaced the primary Ab are negative for HMGB1 staining (red) after PBS (**E**) and VIP (**F**) treatments. (Epithelium=Epi and stroma=Stroma). Mag=115X (n=5/group/time/assay)

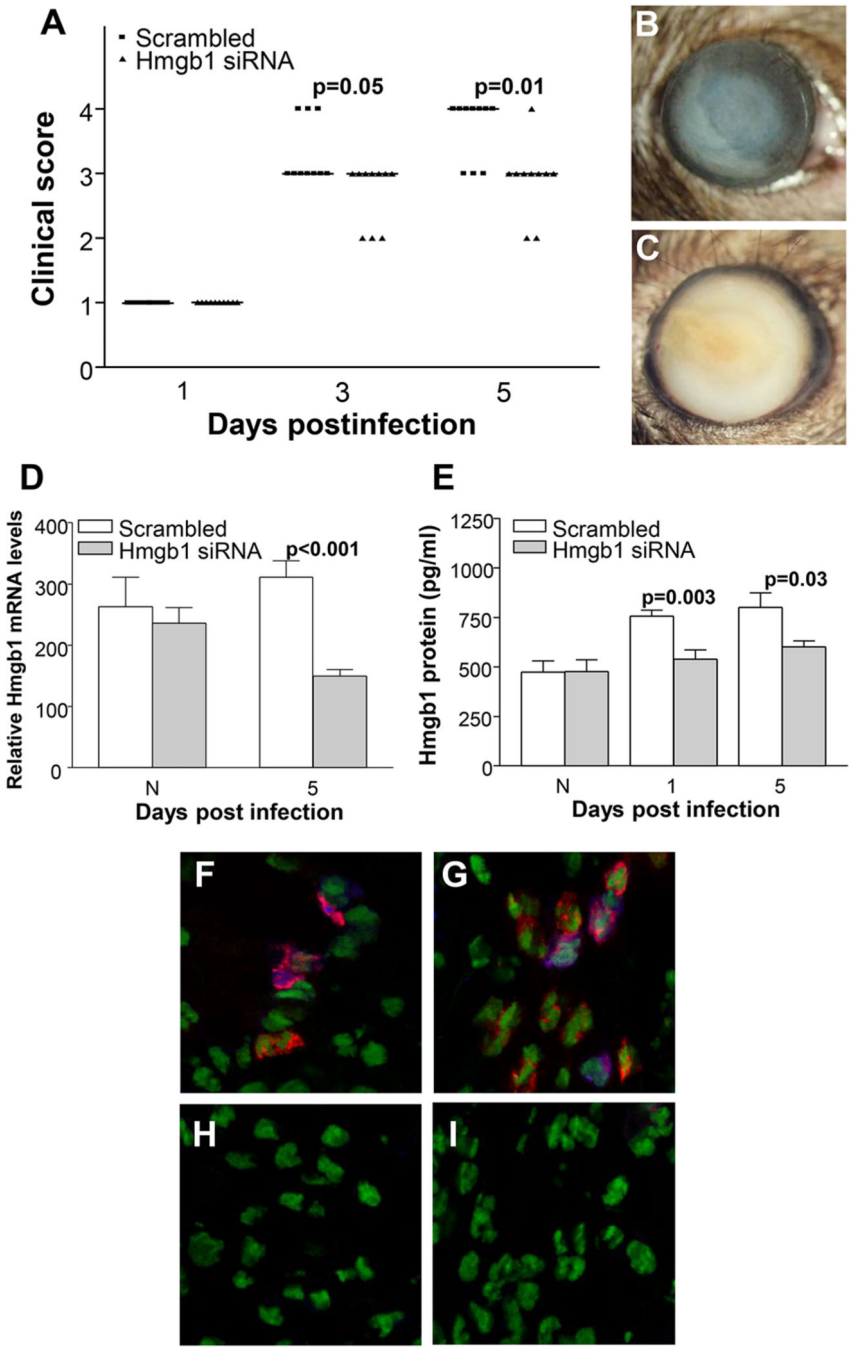

Figure 3. Interference of HMGB1 expression with siRNA

Clinical score (**A**) shows that treatment with siRNA HMGB1 resulted in significantly less disease at 3 and 5 days p.i. (p=0.05 and p=0.01, respectively) with no difference at 1 day p.i. (n=10/group/time). Photographs taken with a slit lamp of representative corneas at 5 days p.i. show less opacity with no corneal perforation in knockdown treated mice (+2 to +3) (**B**) and corneal perforation in the control cornea (+4) (**C**). RT-PCR showed significant down-regulation of HMGB1 mRNA at 5 days p.i after silencing HMGB1 (p<0.001) (**D**), and ELISA assay showed a similar reduction in HMGB1 protein at both 3 and 5 days p.i. after

siHMGB1 treatment (p=0.003 and p=0.03) (**E**). Dual immunohistochemistry (magenta) for HMGB1 (blue) and macrophages (red) (**F**) or PMN (red) (**G**) revealed that both cell types are a source of HMGB1 in the infected cornea. Negative controls in which species specific IgG replaced the primary antibodies are negative (**H** and **I**). Clinical score data (**A**) analyzed using a non-parametric Mann-Whitney test, with medians indicated for each group. Data shown in (**D)** and (**E)** analyzed using a two-tailed Student's t-test and shown as the mean ± SEM. B and C Mag=8X (n=10/group/time), F and I Mag=500X.

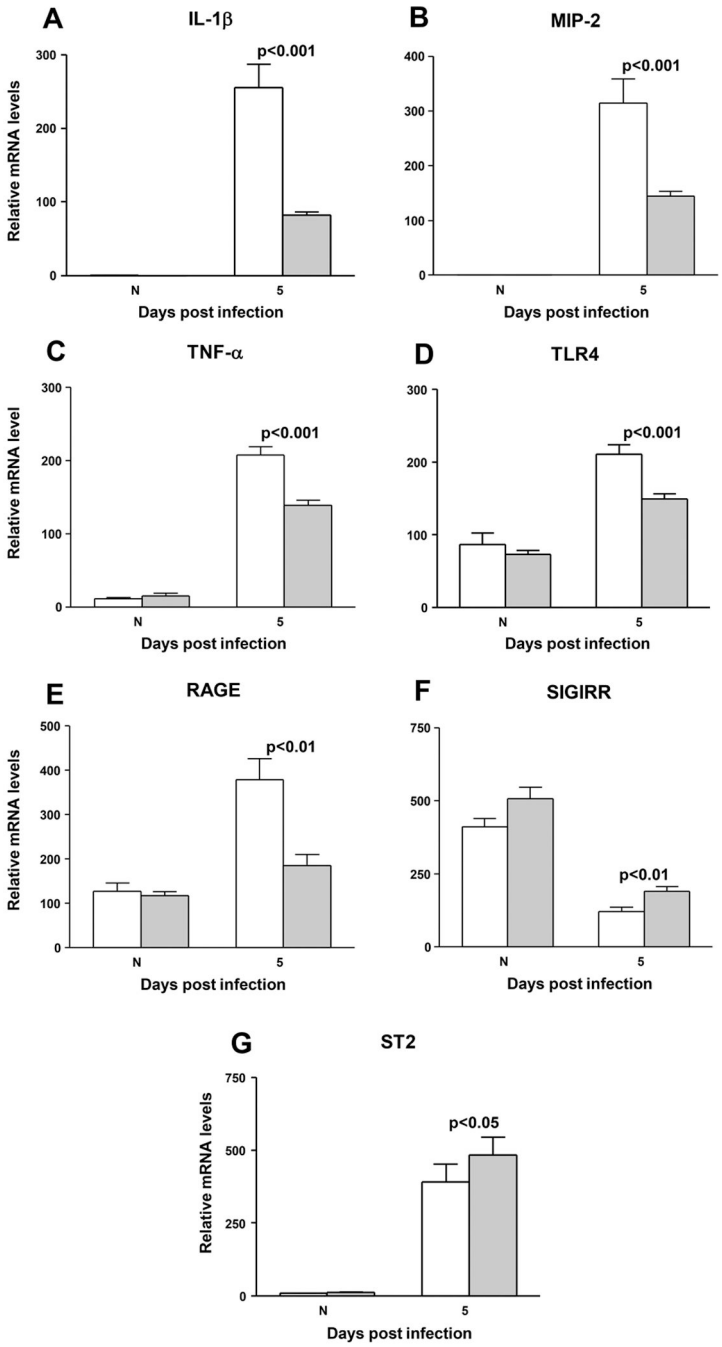

Figure 4. Real time RT-PCR

RT-PCR revealed significantly reduced expression of mRNA for (**A**) IL-1β ($p<0.001$), (**B**) MIP-2 ($p<0.001$), (**C**) TNF-α ($p<0.001$), (**D**) TLR4 ($p<0.001$), and (**E**) RAGE ($p<0.01$) after silencing HMGB1. mRNA expression for (**F**) SIGIRR and (**G**) ST2 were significantly elevated after HMGB1 silencing ($p<0.01$ and 0.05, respectively) (n=5/group/time). Data shown in (**A–G)** analyzed using a two-tailed Student's t-test and shown as the mean ± SEM.

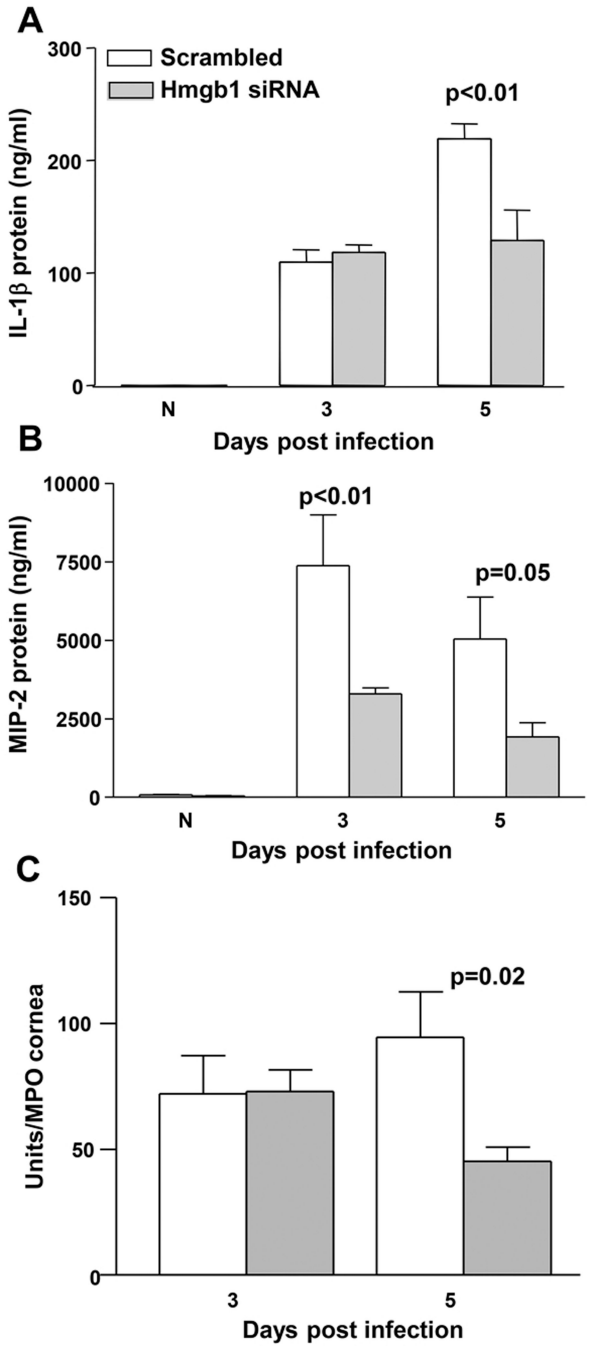

Figure 5. ELISA and MPO assay

Protein levels for IL-1β (**A**) were significantly reduced at 5 days p.i. after silencing HMGB1 compared to scrambled control treatment ($p<0.01$) with no difference seen between groups at 3 days p.i. or in normal, uninfected corneas. Silencing HMGB1 significantly reduced MIP-2 protein levels (**B**) at 3 and 5 days p.i. compared to scrambled controls ($p<0.01$ and $p=0.05$). No difference was detected between groups in normal, uninfected cornea. MPO assay (**C**) detected fewer PMN in the cornea of siHMGB1 vs scrambled control treated mice

(p=0.02). (n=5/group/time for each assay) Data shown in (**A-C)** analyzed using a two-tailed Student's t-test and shown as the mean ± SEM.

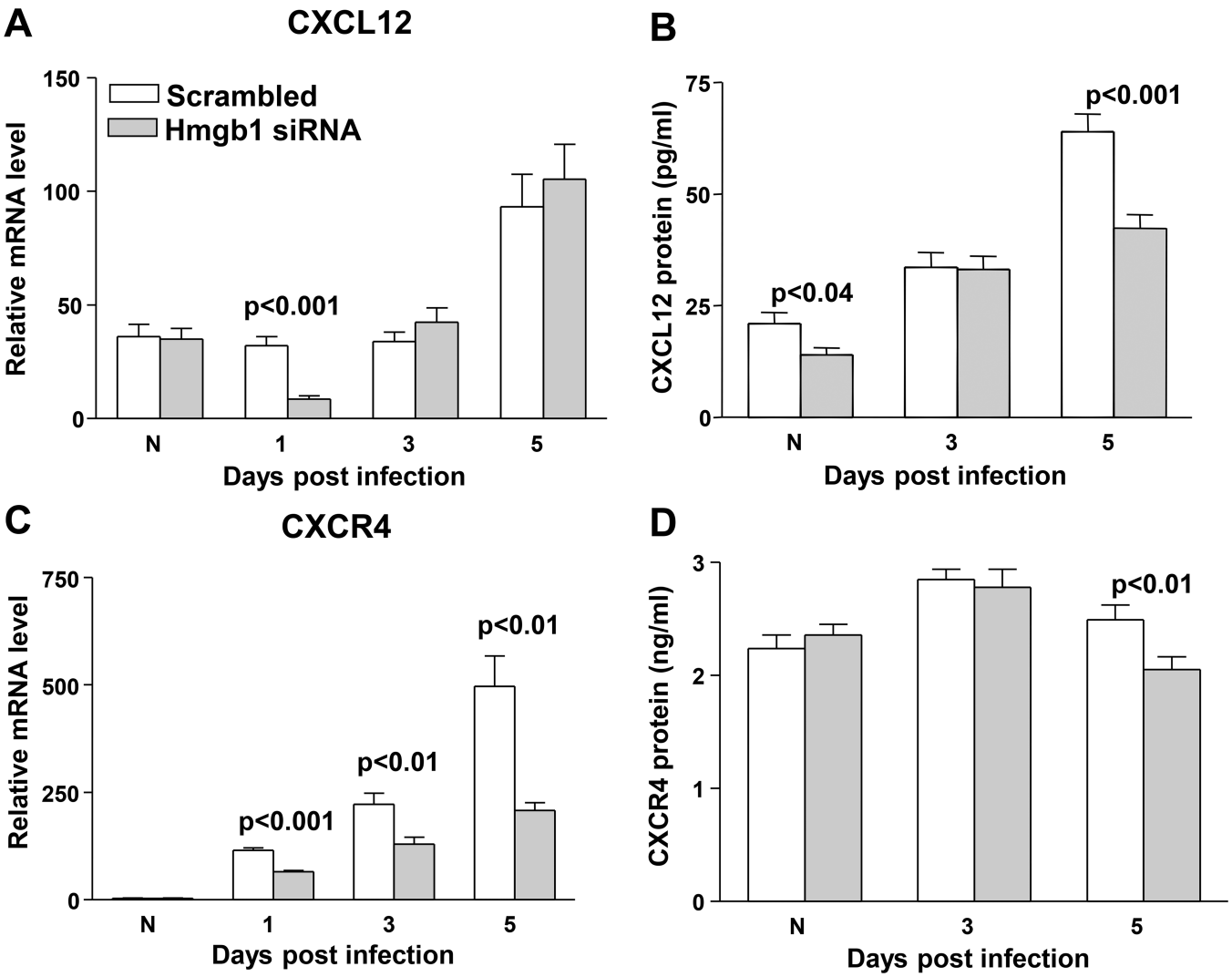

Figure 6. RT-PCR and ELISA for inflammatory cell recruitment complex molecules

(A–E). Significantly less CXCL12 mRNA was detected in the cornea after silencing HMGB1 at 1 day p.i. ($p<0.001$) compared to scrambled siRNA treatment No significant difference was detected between groups in normal, uninfected cornea or at 3 and 5 days p.i. (**A**). CXCL12 protein was reduced in the normal ($p<0.04$) and at 5 days p.i. ($p<0.001$) cornea after siHMGB1 treatment (**B**). Expression of CXCR4 was significantly reduced in the cornea of siHMGB1 compared to scrambled control treated mice at 1, 3, and 5 days p.i. ($p<0.001$, 0.01, and 0.01). No difference was detected between groups in normal, uninfected corneas (**C**). CXCR4 protein was significantly reduced in the corneas of siHMGB1 vs control treated mice at 5 days p.i. ($p<0.01$). No difference was detected between groups in normal, uninfected corneas or at 3 days p.i. (**D**).

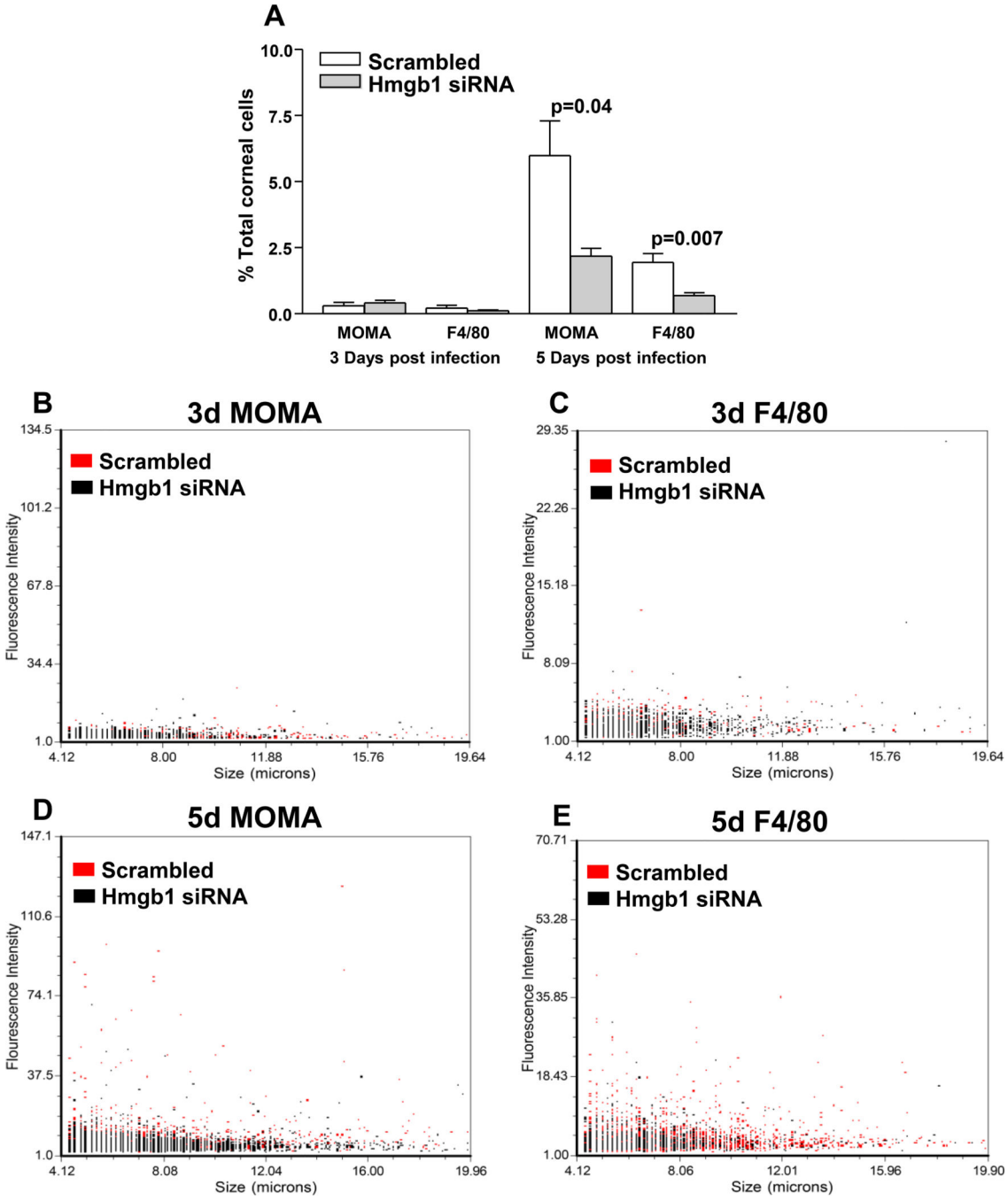

Figure 7. Cell analysis

MOMA and F4/80 positive cells, assayed separately, were no different between groups at 3 days p.i.; at 5 days p.i., fewer MOMA positive (p=0.04) cells and fewer F4/80 positive cells (p=0.007) were seen after siHMGB1 when compared to scrambled control treatment (**A**). (n=5/group/time/assay). Dot plots (**B–E**), show no differences between groups at 3 days, but at 5 days, siHMGB1 treatment reduced intermediate and large size cell populations when compared with scrambled control treatment. Data shown in (**A)** analyzed using a two-tailed Student's t-test and shown as the mean ± SEM.

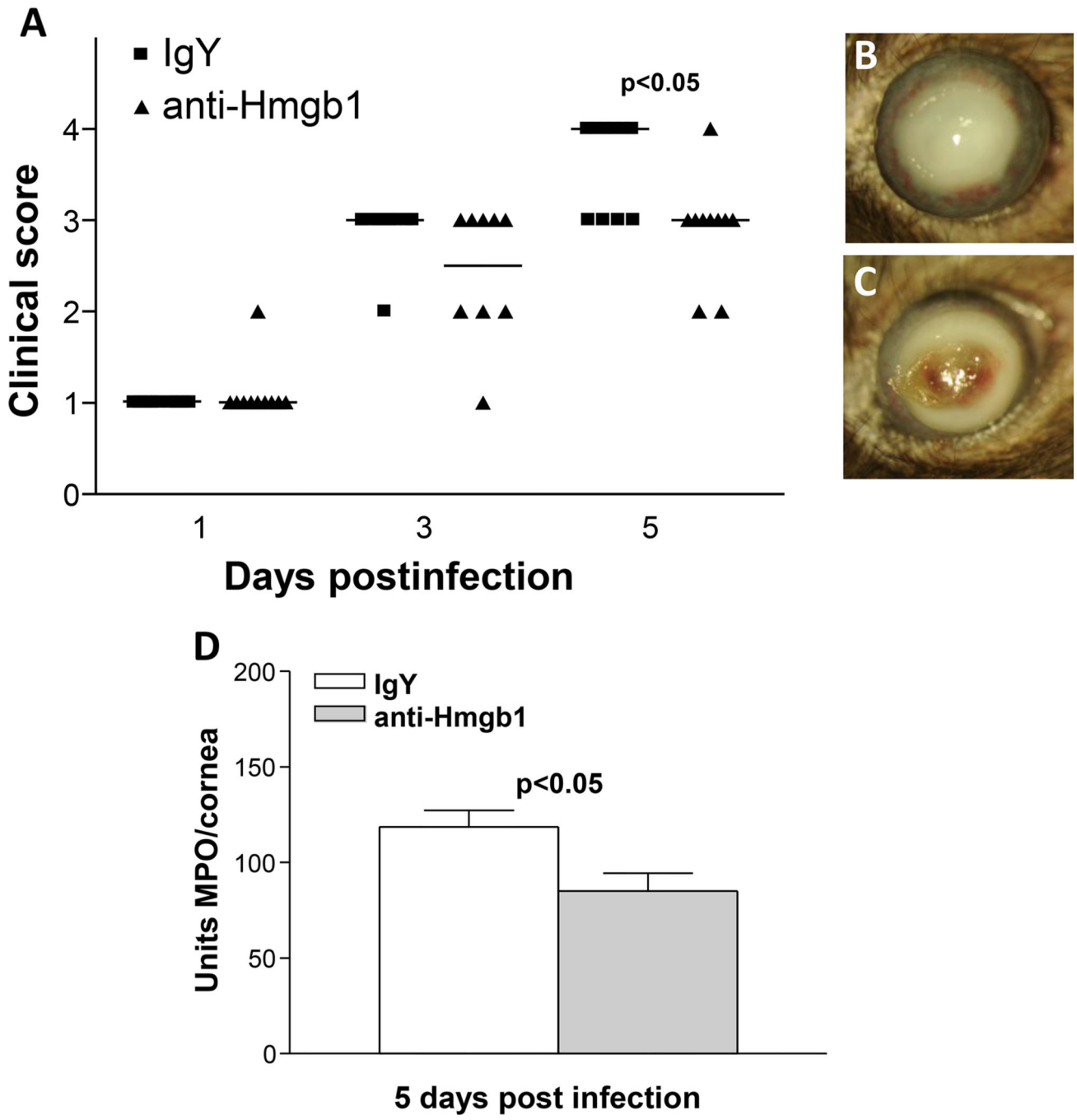

Figure 8. HMGB1 neutralization

Clinical score (**A**) shows that antibody neutralization of HMGB1 resulted in significantly less disease at 5 days p.i. ($p<0.05$) with no difference in disease scores seen at 1 and 3 days p.i. (n=10/group/time). Photographs taken with a slit lamp of representative corneas at 5 days p.i. show opacity with no perforation in the cornea of anti-HMGB1 treated mice (+3) (**B**) and corneal perforation in the IgY treated control cornea (+4) (**C**). MPO assay (**D**) detected fewer PMN in the cornea of anti-HMGB1 vs IgY control treated mice at 5 days p.i. ($p<0.05$) (n=10/group/time for each assay) Clinical score data (**A**) analyzed using a non-

parametric Mann-Whitney test, with medians indicated for each group. Data shown in (**D)** analyzed using a two-tailed Student's t-test and shown as the mean ± SEM. B and C Mag= 5X.

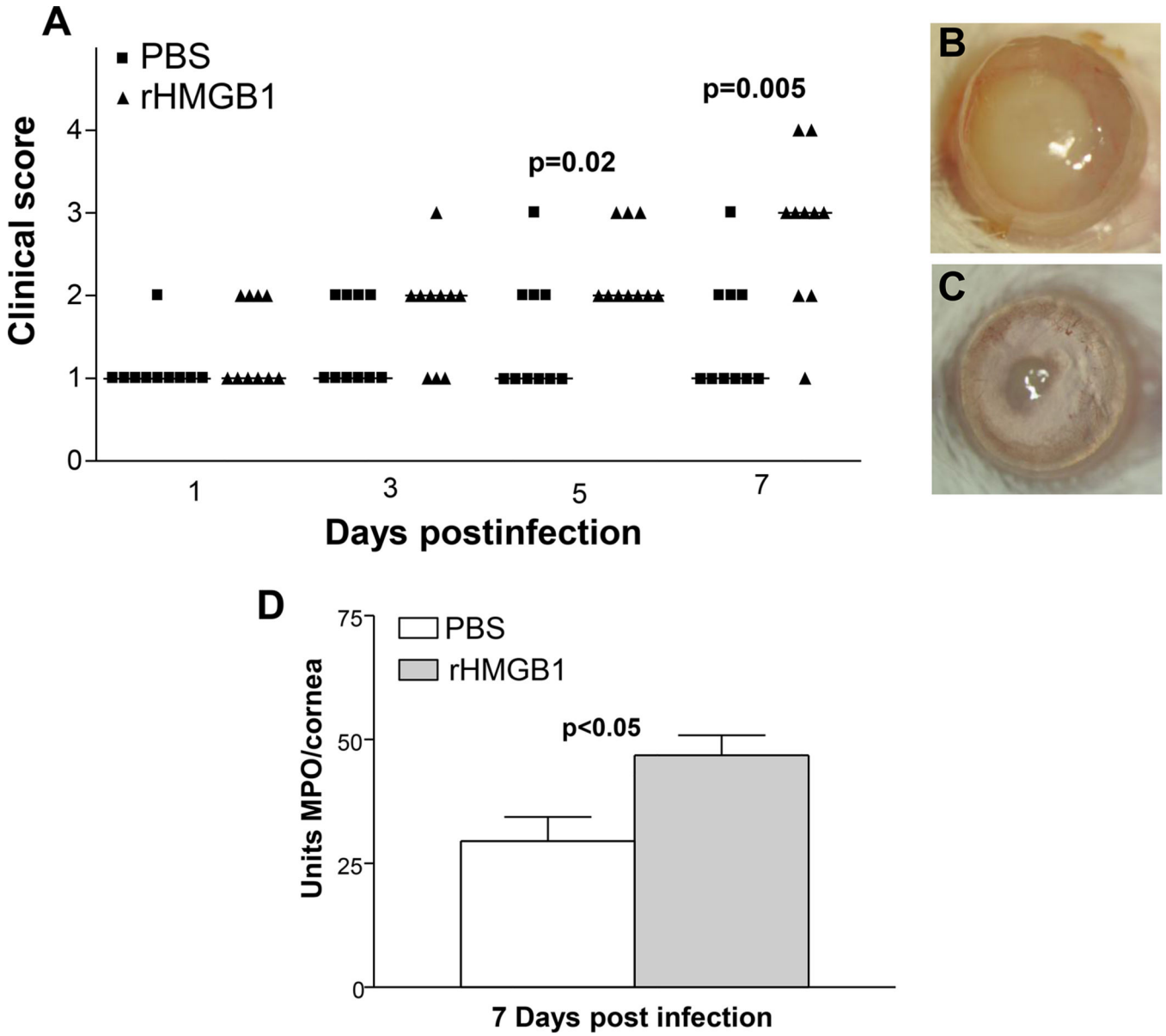

Figure 9. rHMGB1 treatment

Clinical score (**A**) shows that rHMGB1 resulted in significantly more severe disease at 5 and 7 days p.i. (p=0.02 and p=0.005, respectively) with no difference in disease scores at 1 and 3 days p.i. (n=10/group/time). Photographs taken with a slit lamp of representative corneas at 7 days p.i. show more opacity in the cornea of rHMGB1 treated mice (+2 to +3) (**B**) and slight opacity in PBS treated control cornea (0 to +1) (**C**). MPO assay (**D**) detected more PMN in the cornea of rHMGB1 vs PBS control treated mice at 7 days p.i. ($p<0.05$) (n=10/group/time) Clinical score data (**A**) analyzed using a non-parametric Mann-Whitney test, with medians indicated for each group. Data shown in (**D)** analyzed using a two-tailed Student's t-test and shown as the mean ± SEM. B and C Mag=5X.

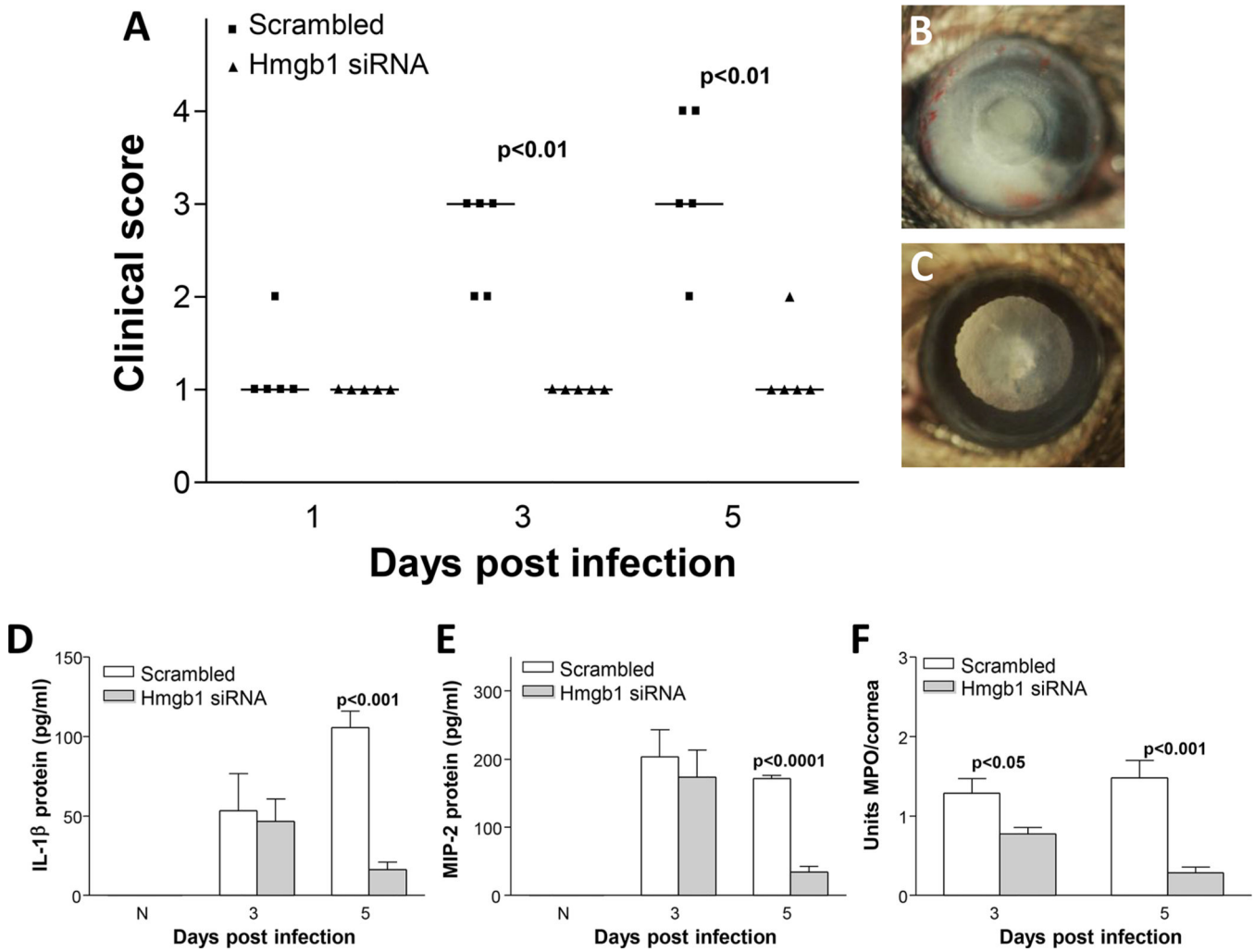

Figure 10. siHMGB1 treatment and infection with clinical isolate KEI 1025

Clinical score (**A**) shows that treatment with siRNA for HMGB1 resulted in significantly less disease at 3 and 5 days p.i. ($p<0.01$ for both) with no difference in disease scores seen at 1 day p.i. (n=5/group/time). Photographs taken with a slit lamp of representative corneas at 5 days p.i. show only slight central opacity in the cornea of knockdown treated mice (+1) (**B**) and a more dense corneal opacity in the control cornea (+2 to +3) (**C**). Protein levels for IL-1β (**D**) were significantly reduced at 5 days p.i. after silencing HMGB1 compared to scrambled control treatment ($p<0.001$) with no difference seen between groups at 3 days p.i. or in normal, uninfected corneas. Silencing HMGB1 significantly reduced MIP-2 protein levels (**E**) 5 days p.i. compared to scrambled controls ($p<0.0001$). No difference was detected between groups at 3 days p.i. or in normal, uninfected cornea. MPO assay (**F**) detected fewer PMN in the cornea of siHMGB1 vs scrambled control treated mice at both 3 and 5 days p.i. ($p<0.05$ and $p<0.001$, respectively). (n=5/group/time for each assay) Clinical score data (**A**) analyzed using a non-parametric Mann-Whitney test, with medians indicated for each group. Data shown in (**D–F)** analyzed using a two-tailed Student's t-test and shown as the mean ± SEM. B and C Mag=6X.

Table I

Nucleotide sequence of the specific primers used for PCR amplification

Gene	Nucleotide Sequence	Primer	GenBank
β-actin	5'- GAT TAC TGC TCT GGC TOC TAG C -3'	F	NM_007393.3
	5'- GAC TCA TOG TAC TOC TGC TTG C -3'	R	
HMGB1	5'- TGG CAA AGG CTG ACA AGG CTC -3'	F	NM_010439.3
	5'- GGA TGC TOG OCT TTG ATT TTG G -3'	R	
IL-1β	5'- OGC AGC AGC ACA TCA ACA AGA GC -3'	F	NM_008361.3
	5'- TGT OCT CAT OCT GGA AGG TOC AOG -3'	R	
MIP-2	5'- TGT CAA TGC CTG AAG AOC CTG OC -3'	F	NM_009140.2
	5'- AAC TTT TTG AOC GOC CTT GAG AGT GG -3'	R	
TNF-α	5'- AOC CTC ACA CTC AGA TCA TCT T -3'	F	NM_013693.2
	5'- GGT TGT CTT TGA GAT OCA TGC -3'	R	
TLR4	5'- OCT GAC AOC AGG AAG CTT GAA -3'	F	NM_021297.2
	5'- TCT GAT OCA TGC ATT GGT AGG T -3'	R	
RAGE	5'- GCT GTA GCT GGT GGT CAG AACA -3'	F	NM_007425.2
	5'- OOC CTT ACA GCT TAG CAC AAG TG -3'	R	
SIGIRR	5'-GTG GCT GAA AGA TGG TCT GGC ATT G -3'	F	NM_023059.3
	5'- CAG GTG AAG GTT OCA TAG TOC TCT GC -3'	R	
ST2	5'- TGA OGC OCA OCA GAT CAT TCA CAG -3'	F	NM_010743.2
	5'- GOC AAA GCA AGC TGA ACA GGC AAT AC -3'	R	
CXCL12	5'- TGC ATC AGT GAC GGT AAA OCA -3'	F	NM_021704.3
	5'- CAC AGT TTG GAG TGT TGA GGA T -3'	R	
CXCR4	5'- CTT CTG GGC AGT TGA TGC CAT -3'	F	NM_009911.3
	5'- CTG TTG GTG GOG TGG ACA AT -3'	R	

F, forward; R, reverse.